



Internal rotation and intramolecular hydrogen bonding in thiosalicylamide: gas phase electron diffraction study supported by quantum chemical calculations

Inna N. Kolesnikova¹ · Anatolii N. Rykov¹ · Maxim V. Shuvalov¹ · Igor F. Shishkov¹

Received: 19 March 2019 / Accepted: 30 May 2019
© Springer Science+Business Media, LLC, part of Springer Nature 2019

Abstract

The molecular structure of thiosalicylamide (2-hydroxythiobenzamide) was investigated in the gas phase at 401 K by means of gas electron diffraction (GED) combined with quantum chemical (QC) calculations. Special attention was paid to the internal rotation of the thioamide group. Structural refinement was performed taking into account rovibrational corrections to the thermal-average internuclear distances calculated with harmonic and anharmonic (cubic) MP2/cc-pVTZ force constants in terms of static and dynamic models. It was shown that both models fitted the GED data equally well. The results of the GED refinement revealed that in the equilibrium structure, the thioamide group is twisted by about 30° with respect to the phenol ring plane. This is the result of an interatomic repulsion of hydrogen atom in the amide group from the closest hydrogen atom of the benzene ring, which overcomes the energy gain from the π - π conjugation of the thioamide group and the aromatic system of thiosalicylamide. Natural bond orbital (NBO) analysis and comparison of the thiosalicylamide molecular structure with those of related compounds revealed hydrogen-bonded fragment between the hydroxyl and thiocarbonyl groups. The structure of thiosalicylamide in the gas phase was found to be markedly different from that in the solid phase due to the effect of intermolecular hydrogen bonding in the crystal.

Keywords Thiosalicylamide · 2-Hydroxythiobenzamide · Molecular structure · Gas electron diffraction · Quantum chemistry · Internal rotation · Intramolecular hydrogen bonding

Introduction

Salicylamides and thiosalicylamides are compounds of special interest in medicinal chemistry [1–5]. While the molecule structure of salicylamide, a well-known non-prescription antiseptic drug, has been extensively studied [6–11], data are scarce concerning the structure and conformation of its bioisosteric sulfur-containing analog, thiosalicylamide (Fig. 1). The molecular structure of thiosalicylamide in the solid phase was determined by means of X-ray diffraction

(XRD) [7]. According to XRD, the asymmetric unit of thiosalicylamide contains two crystallographically independent molecules with similar molecular parameters. Two types of hydrogen bonds are present in the crystal phase: intramolecular O–H...S bonds ($r_{\text{H...S}} \sim 2.0 \text{ \AA}$) and intermolecular N–H...S and N–H...O bonds ($r_{\text{H...S}} \sim 2.6 \text{ \AA}$ and $r_{\text{H...O}} \sim 2.1 \text{ \AA}$). The investigation of the structural properties of thiosalicylamide and its metal complexes made by means of IR spectroscopy confirmed that the OH group is bonded in the solid state [12]. Unlike salicylamide which is almost flat in the crystal phase, the thioamide group in thiosalicylamide is twisted by approximately 20° relative to the plane of the ring [7]. While theoretical investigations of free molecules were performed for a few compounds similar to thiosalicylamide, such as 4-hydroxythiobenzamide [13] and 2-hydroxy-N-methylthiobenzamide [14], neither computational nor experimental data could be found for the gaseous structure of thiosalicylamide. Thus, steric effect of the large sulfur atom on the conformation of gaseous thiosalicylamide molecule in comparison with its oxo-analog has remained unknown.

Electronic supplementary material The online version of this article (<https://doi.org/10.1007/s11224-019-01369-y>) contains supplementary material, which is available to authorized users.

✉ Inna N. Kolesnikova
i_n_kolesnikova@mail.ru

¹ Chemistry Department, Lomonosov Moscow State University, Leninsky Gory 1, Moscow, Russian Federation 119991

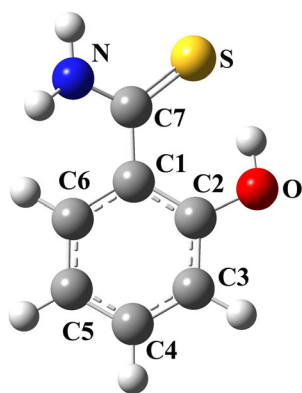


Fig. 1 Structural formula of thiosalicylamide and the numbering of atoms

This report is aimed to fill this gap and presents the first study of thiosalicylamide molecular structure in the gas phase by means of gas electron diffraction (GED) supported by quantum chemical (QC) calculations. The obtained results are used to discuss the structural changes caused by the replacement of oxygen atom in salicylamide by the larger and less electronegative sulfur and the effect of intermolecular hydrogen bonding on the structure of thiosalicylamide in the crystal phase.

Experimental section

Syntheses of thiosalicylamide

Salicylamide (0.5 g, 4.4 mmol) and Lawesson's reagent (1 g, 2.5 mmol) were stirred in tetrahydrofuran (4 mL) under Ar atmosphere at 55 °C within for 4 h. After aluminum oxide (10 g) was added to the mixture, the solvent was evaporated in vacuum. Thiosalicylamide was eluted from the resulting solid with acetonitril–ethanol (10:1) using column chromatography. The yield was 50%, m. p. 118–119 °C (cf. Ref. [15]; m. p. 119–120 °C). The purity of the substance was confirmed by NMR spectra recorded in a Bruker Avance 400 NMR spectrometer in CDCl₃ at frequencies 400.13 MHz (¹H) and 100.61 MHz (¹³C) using SiMe₄ as internal standard. The following chemical shifts (δ , ppm) were observed in ¹H NMR: 6.88 (t, 1H, C₆H₅, J = 7.69 Hz), 7.05 (d, 1H, C₆H₅, J = 8.47 Hz), 7.41 (m, 1H, C₆H₅), 7.46 (broad s, 2H, NH₂), 7.61 (m, 1H, C₆H₅), 11.7 (broad s, 1H, OH), and ¹³C NMR: 119.2(C₃), 119.6(C₁), 119.9(C₅), 124.2 (C₆), 134.8 (C₄), 160.2 (C₂), 198.4 (C=S).

GED experiment

The GED patterns of thiosalicylamide were recorded in an electron diffraction apparatus EG-100 M at long (36 cm) and short (19 cm) camera distances (LD and SD, respectively) on

MACO EM-FILM EMS photo films. The details of the GED experiments are given in Table 1.

An Epson Perfection 4870 photo scanner was used to process the films with recorded diffraction patterns in order to obtain digital images of GED data in 16-bit/600-dpi gray scale. The resulting data for LD and SD were transformed into mean optical density functions of s , with an increment of 0.2 Å⁻¹ by applying the PLATE program [16]. The experimental intensity curves are presented in Fig. 2, which also displays the background lines $B(s)$ obtained for a dynamic model. The background curves for a static model are given in Fig. S1 of the Electronic Supplementary Material (ESM).

QC calculations

Computational programs and methods

All QC calculations presented in this work were made using Gaussian03 software [17]. The methods were B3LYP [18, 19] and MP2 [20] including basis sets 6-31G(d,p) [21] and cc-pVTZ [22], with appropriate scale factors (http://cccbas.nist.gov/vibscalejust.asp). The natural bond orbitals (NBO) analysis [23] was performed with the NBO program integrated in Gaussian03. The program ChemCraft [24] was used for visualization of molecular orbitals.

Scans of potential energy

In order to find possible conformers of thiosalicylamide, two-dimensional potential energy surface (PES) scan for simultaneous internal rotation of the thioamide and the hydroxyl groups was performed at the B3LYP/6-31 G(d,p) level of theory (Fig. 3). The internal coordinate describing internal rotation of the thioamide group was the dihedral angle φ_1 (C2–C1–C7–S) and the scanned coordinate for the hydroxyl group was the dihedral φ_2 (C1–C2–O–H). Both dihedral angles φ_1 and φ_2 were changed in steps of 10°.

Table 1 Summary of the GED experiments

	LD	SD
T, K	398	403
I _{electron beam} , μ A	2.2	2.8
$\lambda_{\text{electrons}}$ ^a , Å	0.049708	0.049850
s range ^b , Å ⁻¹	3.0–18.4	7.6–31.6
P _{residual gas} , Pa	4.0·10 ⁻³	3.0·10 ⁻³
Number of photo films	3	3

^a The electron wavelength was calibrated against gaseous CCl₄

^b $s = \frac{4\pi r \sin \theta}{\lambda_{\text{electrons}}}$ with scattering angle $\theta = \arctan \frac{r}{D}$, where r is the distance from the center of the plate and D is the nozzle-to-plate distance

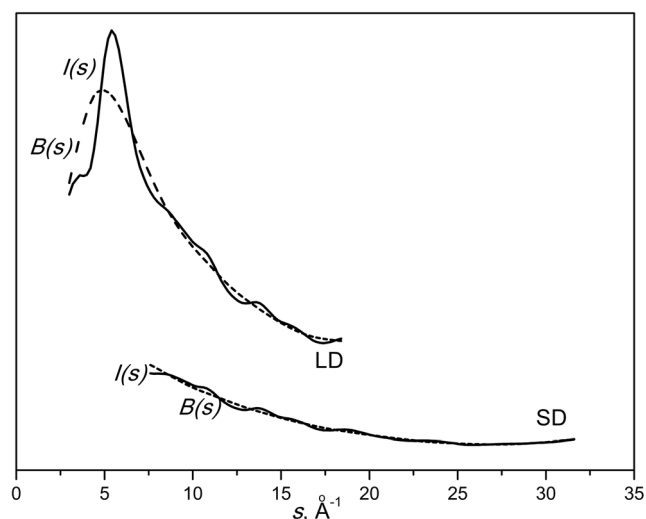


Fig. 2 Experimental intensity curves and background lines for thiosalicylamide

Additional one-dimensional scans for internal rotation of the thioamide group were performed for the lowest energy form at B3LYP/cc-pVTZ and MP2/cc-pVTZ levels of theory; the scanned angle φ_1 was varied in steps of 10° (Fig. 4). It is noteworthy that the $E(\varphi_1) = E(-\varphi_1)$ symmetry exists.

Optimizations of conformers

For all the minima detected on the two-dimensional PES, the geometries were fully optimized at B3LYP/6-31G(d,p), B3LYP/cc-pVTZ, and MP2/cc-pVTZ, using the *opt = tight* and *int = ultrafine* parameters. The harmonic vibration frequencies were calculated at the same levels of theory to characterize the optimized stationary points and to confirm that negative eigenvalues are absent in the Hessian matrix. The optimized Cartesian coordinates of all thiosalicylamide conformers obtained at the different levels of theory are available in the ESM (Tables S1–S10).

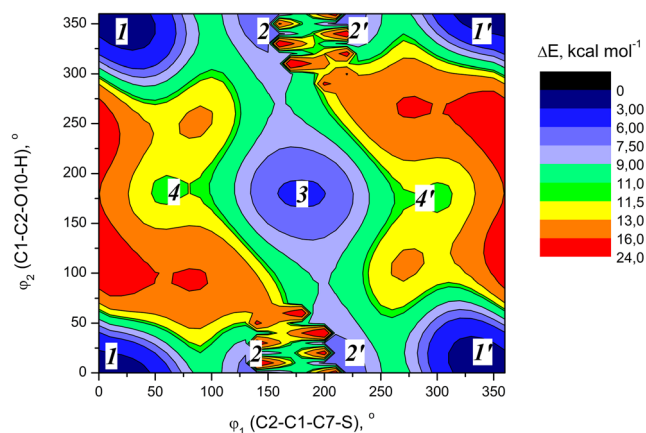


Fig. 3 Potential energy surface for internal rotation of the thioamide (φ_1) and the hydroxyl groups (φ_2) in thiosalicylamide

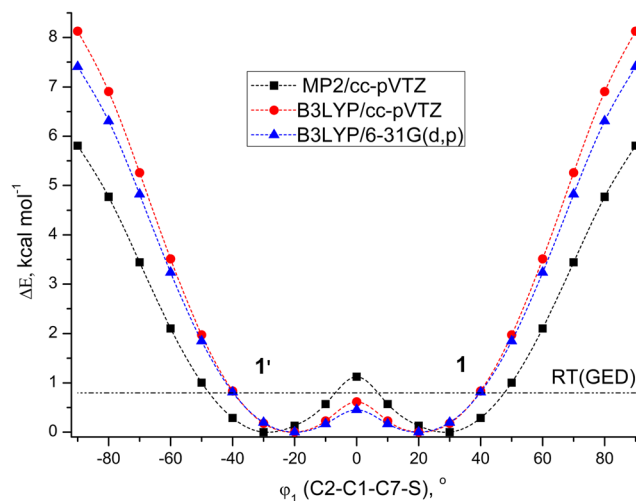


Fig. 4 Relaxed scans for rotation of the thioamide group around the C1–C7 bond in thiosalicylamide using QC calculations

According to the results B3LYP/6-31G(d,p), four conformers of thiosalicylamide with different orientations of the thioamide and the hydroxyl groups are possible in the gas phase (Fig. 5). Note that conformers **1**, **2**, and **4** have enantiomeric isomers **1'**, **2'**, and **4'**, respectively, since they possess C_1 symmetry, while conformer **3** possessing C_s symmetry is single.

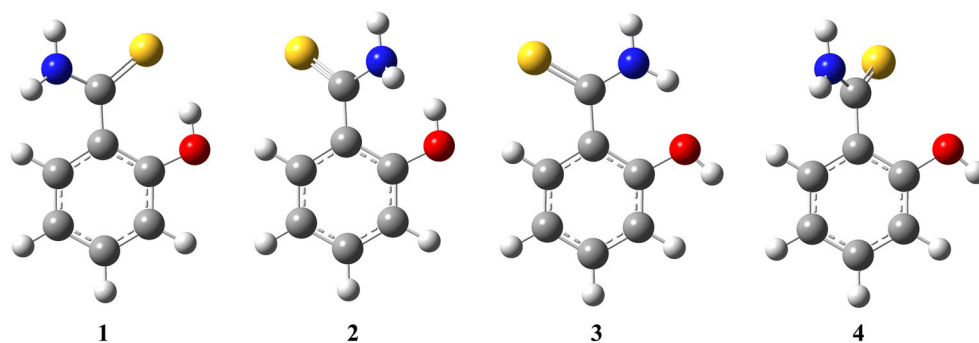
However, B3LYP/cc-pVTZ and MP2/cc-pVTZ computations do not confirm that conformer **4** is possible the gas phase, and MP2/cc-pVTZ method predicts C_1 symmetry for conformer **3**. The energy differences between conformers and their distribution at 401 K (the average temperature of the GED experiment) at various levels of theory are given in Table 2. All computations show that conformer **1** is predominant in the gas phase (more than 99%).

A low energy barrier to rotation about the C1–C7 bond separates two optical isomers **1** and **1'** (see Fig. 4). It is estimated to be ~ 1 kcal mol $^{-1}$ according to QC calculations and is comparable with the average thermal energy of the internal rotation mode $RT = 0.80$ kcal mol $^{-1}$. The thioamide group torsion vibration is estimated to be less than 100 cm $^{-1}$ (ca. 61 cm $^{-1}$, 56 cm $^{-1}$, and 57 cm $^{-1}$ according to B3LYP/6-31G(d,p), B3LYP/cc-pVTZ, and MP2/cc-pVTZ calculations, respectively). Thus, the results of QC calculations indicate that only the lowest energy form (conformer **1**) should be considered in the GED analysis. Moreover, the flexibility of conformer **1** makes it reasonable to interpret the GED data in terms of a dynamic model. To consider the thioamide torsion group vibration as a large-amplitude motion, the additional QC calculations were performed for pseudo-conformers with the dihedral angle φ_1 (C2–C1–C7–S) ranging from 0 to 60°.

Pseudo-conformers optimizations

The geometries of thiosalicylamide pseudo-conformers were optimized at MP2/cc-pVTZ level of theory using the *opt =*

Fig. 5 Conformers of thiosalicylamide (optical isomers are not shown)



tight and *int = ultrafine* parameters and option *frozen* for the dihedral angle φ_1 . Subsequent frequency calculations were performed at the same level of theory. The optimized Cartesian coordinates of thiosalicylamide pseudo-conformers are available in Section 1 of the ESM (Tables S11–S16). Note that pseudo-conformer with $\varphi_1 = 0^\circ$ possesses C_s symmetry and has one imaginary vibrational frequency ($\nu(A'')_{43} = -158 \text{ cm}^{-1}$) as it corresponds to a transitional state for internal rotation.

Structure refinements

General considerations

The structure of thiosalicylamide was refined in terms of static (rigid) and dynamic models using UNEX program [25]. The function that was minimized had a standard form and a criterion of minimum of the functional served *R*-factor [26]. The initial geometrical parameters of thiosalicylamide were taken from the results of QC computations at MP2/cc-pVTZ level of theory and the vibrational parameters (the mean square amplitudes of atom pairs *l* and shrinkage corrections $r_e - r_a$ [27]) were derived from quadratic and cubic force fields obtained at

the same level of theory applying VibModule program [28]. During the refinement procedure, some of the independent equilibrium structural parameters (bond lengths, bond, and dihedral angles) were combined in groups as indicated in Table 3. The differences between the parameters in groups were fixed at quantum-chemical values. Estimated standard deviations for the refined parameters were multiplied by a factor of three in order to include possible uncertainties due to data correlation and scale uncertainty [26]. Note that geometrical parameters involving hydrogen atoms were kept equal to theoretical values due to a weak sensitivity of GED to the positions of hydrogens [29]. The mean vibrational amplitudes were fixed at theoretical values.

Static model

The refinement was performed with an assumption that only the lowest energy form of thiosalicylamide (conformer **1**) is present in the gas phase as it had been predicted by QC computations. The conventional algorithm of structural analysis for a molecule undergoing small-amplitude vibrations was applied [26]. The contribution of the all vibration frequencies including the lowest energy vibration were used to derive the amplitudes of vibrations and the vibration corrections. The

Table 2 Relative total electronic energies^a, relative standard Gibbs free energies^b, and percentage abundances^c for thiosalicylamide conformers at the average temperature of the GED experiment

Method	Conformer	Symmetry	ΔE (kcal mol ⁻¹)	ΔG°_{401} (kcal mol ⁻¹)	P ₄₀₁ (%)
B3LYP/6-31G(d,p)	1	C ₁	0.00	0.00	99.5
	2	C ₁	5.75	5.72	0.1
	3	C _s	4.81	4.42	0.4
	4	C ₁	8.99	7.95	$5 \cdot 10^{-3}$
B3LYP/cc-pVTZ	1	C ₁	0.00	0.00	99.2
	2	C ₁	6.22	6.15	$4 \cdot 10^{-2}$
	3	C _s	5.35	3.89	0.8
MP2/cc-pVTZ	1	C ₁	0.00	0.00	99.3
	2	C ₁	4.67	4.58	0.3
	3	C ₁	4.98	4.35	0.4

^a The corresponding values contain ZPVE correction

^b For conformers with C₁ symmetry, which are present as an equimolar mixture of the two optical isomers ΔG°_{401} includes the entropy of mixing (Rln2)

^c The corresponding values are obtained using Boltzmann equation

Table 3 Bond distances (r , Å), bond, and dihedral angles (\angle , °) of thiosalicylamide obtained by various methods

Parameters	GED ^a		XRD[7] ^b		B3LYP/		MP2/
	Static model	Dynamic model	I	II	6-31G(d,p)	cc-pVTZ	cc-pVTZ
$r(\text{C}_1\text{---}\text{C}_2)$	1.409(2) ¹	1.405(2) ¹	1.401(5)	1.389(5)	1.427	1.421	1.415
$r(\text{C}_2\text{---}\text{C}_3)$	1.395(2) ¹	1.391(2) ¹	1.417(5)	1.394(5)	1.408	1.402	1.400
$r(\text{C}_3\text{---}\text{C}_4)$	1.379(2) ¹	1.376(2) ¹	1.350(5)	1.352(7)	1.383	1.377	1.385
$r(\text{C}_4\text{---}\text{C}_5)$	1.391(2) ¹	1.387(2) ¹	1.379(7)	1.375(7)	1.403	1.397	1.396
$r(\text{C}_5\text{---}\text{C}_6)$	1.379(2) ¹	1.376(2) ¹	1.384(5)	1.384(3)	1.383	1.378	1.385
$r(\text{C}_6\text{---}\text{C}_1)$	1.403(2) ¹	1.399(2) ¹	1.388(5)	1.404(5)	1.417	1.411	1.408
$r(\text{C}-\text{C})$	1.463(7) ²	1.460(7) ²	1.490(5)	1.489(2)	1.473	1.470	1.473
$r(\text{C}-\text{N})$	1.347(12) ³	1.351(12) ³	1.311(4)	1.308(4)	1.351	1.346	1.347
$r(\text{C}=\text{S})$	1.670(3) ⁴	1.668(4) ⁴	1.687(4)	1.684(4)	1.692	1.685	1.664
$r(\text{C}-\text{H})_{\text{av}}$	1.081 ^c	1.081 ^c	0.95(3)	0.96(4)	1.086	1.081	1.081
$r(\text{N}-\text{H})_{\text{av}}$	1.006 ^c	1.006 ^c	1.00(4)	0.91(4)	1.009	1.005	1.006
$r(\text{C}-\text{O})$	1.335(9) ⁵	1.332(7) ⁵	1.347(4)	1.370(4)	1.337	1.335	1.343
$r(\text{O}-\text{H})$	0.985 ^c	0.985 ^c	1.04(4)	0.91(3)	0.993	0.991	0.985
$\angle\text{C}_1\text{C}_2\text{C}_3$	119.0(2) ⁶	119.0(2) ⁶	119.3(3)	120.3(3)	119.4	119.4	119.1
$\angle\text{C}_2\text{C}_3\text{C}_4$	121.2(2) ⁶	121.3(2) ⁶	120.6(4)	120.3(4)	121.2	121.2	121.3
$\angle\text{C}_3\text{C}_4\text{C}_5$	120.4(8) ^d	120.4(7) ^d	121.1(4)	120.8(4)	120.3	120.2	120.0
$\angle\text{C}_4\text{C}_5\text{C}_6$	118.7(9) ^d	118.7(9) ^d	118.8(4)	119.6(4)	119.1	119.1	119.3
$\angle\text{C}_5\text{C}_6\text{C}_1$	122.1(8) ^d	122.2(8) ^d	122.2(4)	121.9(4)	122.4	122.5	121.8
$\angle\text{C}_6\text{C}_1\text{C}_2$	118.3(2) ⁶	118.3(2) ⁶	117.9(3)	117.0(3)	117.5	117.4	118.4
$\angle\text{C}_2\text{C}_1\text{C}_7$	122.3(2) ⁶	122.2(2) ⁶	122.7(3)	122.5(3)	122.7	122.8	122.3
$\angle\text{C}_1\text{C}_7\text{S}_8$	125.6(5) ⁷	125.2(5) ⁷	123.4(3)	123.4(3)	125.1	125.0	124.7
$\angle\text{C}_1\text{C}_7\text{N}_7$	116.3(8) ⁸	116.3(8) ⁸	117.1(3)	117.3(3)	116.6	116.7	115.2
$\angle\text{S}_8\text{C}_7\text{N}_7$	118.1(9) ^d	118.4(9) ^d	119.4(3)	119.3(3)	118.3	118.2	120.1
$\angle\text{C}_1\text{C}_2\text{O}_{10}$	123.6(6) ⁹	123.0(5) ⁹	124.8(3)	123.8(3)	124.7	124.5	124.4
$\angle\text{H}_{16}\text{N}_7\text{H}_{17}$	119.3 ^c	119.3 ^c	122(3)	110(3)	118.4	118.5	119.3
$\angle\text{C}_1\text{C}_2\text{C}_3\text{C}_4$	2.5 ^c	2.5 ^c	1.4(6)	-2.4(6)	2.5	2.4	2.5
$\angle\text{C}_2\text{C}_3\text{C}_4\text{C}_5$	0.2 ^c	0.2 ^c	-0.8(6)	-0.6(6)	0.2	0.1	0.2
$\angle\text{C}_2\text{C}_1\text{C}_7\text{S}_8$	31(3) ¹⁰	28.3 ^c	19.4(3)	-19.4(5)	21.2	20.3	28.3
$\angle\text{C}_6\text{C}_1\text{C}_7\text{N}_7$	28(3) ¹⁰	25.9 ^c	19.0(5)	-18.9(5)	19.3	18.7	25.9
$\angle\text{C}_7\text{S}_8\text{N}_7\text{H}_{16}$	177.9 ^c	177.9 ^c	-177(2)	177(3)	177.9	178.3	177.9
$\angle\text{C}_7\text{S}_8\text{N}_7\text{H}_{17}$	14.0 ^c	14.0 ^c	-2(3)	-13(3)	15.3	13.3	14.0
R_{LD}	3.9	3.4					
R_{SD}	5.1	5.6					
R_{tot}	4.4	4.4					

^a For the GED study, equilibrium parameters (r_e , \angle_e) are presented, R -factors are in %

^b For the XRD study, geometrical parameters are given for the both independent molecules (**I** and **II**) of the unit cell

^c Assumed at the values of MP2/cc-pVTZ calculations

^d Dependent parameters

¹⁻¹⁰ The same numerical superscript indicates the refinement in one group

corresponding values of l and $\Delta(r_a - r_e)$ used in the refinement for static model can be found in the ESM (Table S17). As a result of the refinement, the equilibrium structural parameters of thiosalicylamide were obtained, see Table 3; the corresponding Cartesian coordinates can be found in the Table S18 of the ESM. The disagreement factor appeared to

be 4.4%. The matrix of correlations for a static model is deposited as Table S19 in the ESM. The plots of the experimental and theoretical molecular intensities $sM(s)$ along with their difference curve as well as the plots of the experimental and theoretical radial distributions $f(r)$ with their difference curve can be found in the ESM as Figs. S2 and S3, respectively.

The possibility of the GED method to distinguish different conformers of thiosalicylamide was demonstrated by considering the other forms (conformer **2** and conformer **3**) in the refinements. The values of *R*-factor exceeded 9.0% in the both cases. The corresponding *sM*(*s*) functions are presented in the ESM as Figs. S4 and S5, respectively. A model of a mixture of conformers **1** and **2** was also taken into account. However, after the refinement procedure independent of the starting value of percent abundance of conformer **2**, the amount of conformer **1** always reached 100%.

Dynamic model

As it has been predicted by QC calculations, enantiomers **1** and **1'** are separated by a relatively low energy barrier (see Fig. 4) and a significant fraction of the molecules in the molecular beam would have sufficient energy to pass over the barrier at the temperature of the GED experiment. Therefore, an algorithm derived for molecules undergoing large-amplitude vibrations should be applied.

To consider a large-amplitude motion of the thioamide group, the structure of thiosalicylamide was modeled by seven pseudo-conformers, which include conformer **1** ($\varphi_1 = 28.3^\circ$), three pseudo-conformers with $\varphi_1 < 28.3^\circ$ ($\varphi_1 = 0^\circ, 10^\circ, 20^\circ$), and three pseudo-conformers with $\varphi_1 > 28.3^\circ$ ($\varphi_1 = 40^\circ, 50^\circ, \text{ and } 60^\circ$). Since $E(\varphi_1) = E(-\varphi_1)$, statistical weight of two was used for all pseudo-conformers, except C_s pseudo-conformer ($\varphi_1 = 0^\circ$) for which a statistical weight of one was applied. The vibrational amplitudes and anharmonic corrections for each pseudo-conformer were calculated by including the contributions from all normal modes except the lowest vibrational mode. The obtained data for conformer **1** calculated without the contribution of the lowest energy vibration can be found in the ESM (Table S20). Structural parameters of each of the pseudo-conformers were refined simultaneously with the corresponding parameters of equilibrium configuration (conformer **1**), assuming differences between them at the values from the MP2/cc-pVTZ calculations.

The potential function for torsion vibration of thioamide group was refined in the form

$$V(\varphi_1) = V_0 + \sum_{k=1}^2 \frac{V_{2k}}{2} (1 - \cos(2k\varphi_1))$$

The parameters V_2 and V_4 were varied independently; the V_0 constant was adjusted from the condition $V(\varphi_1) \geq 0$. Refinement of this model converged to give an *R*-factor of 4.4%. After the refinement procedure, the resulting PES parameters for torsion vibration of the thioamide group were estimated to have the following values: $V_0 = 1.2$ kcal/mol, $V_2 = -5.8(8)$ kcal/mol, and $V_4 = 3.6(4)$ kcal/mol. The relative abundance of each pseudo-conformer calculated according to

a Boltzmann equation can be found in Table S21 of the ESM. The refined equilibrium parameters of thiosalicylamide ($\varphi_1 = 28.3^\circ$) from a dynamic model are presented in Table 3; the corresponding Cartesian coordinates can be found in Table S22 of the ESM. The matrix of correlations is given in Table S23 of the ESM. The reduced scattering intensity curves and the radial distribution curve are shown in Figs. 6 and 7, respectively.

Results and discussion

As it can be seen from Table 3, a dynamic model does not significantly improve the quality of the experimental analysis comparing with a static model: structural parameters, experimental uncertainties, and disagreement factors are quite similar in both cases (see Table 3). The usage of a dynamic model for the description of a large-amplitude motion of the thioamide group allowed to refine the potential function parameters.

In general, the geometry of thiosalicylamide molecule is better predicted by means of MP2/cc-pVTZ than by means of B3LYP/6-31G(d,p) and B3LYP/cc-pVTZ methods (see Table 3). For example, B3LYP/6-31G(d,p) overestimates the value of the C=S bond by approximately 0.02 Å and underestimates the angular twist of the thioamide group relative to the benzene ring plane by approximately 10°; however, this method better predicts the value of the C–O bond length and the values of the SCN and the C_1C_7N valence angles than MP2/cc-pVTZ (see Table 3).

The joint GED and QC analysis established that thiosalicylamide possesses a non-planar structure with the thioamide group being twisted by angle $\sim 30^\circ$ with respect

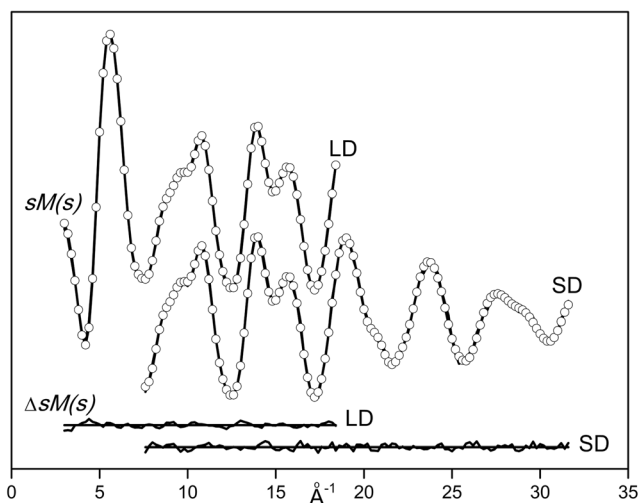


Fig. 6 Reduced molecular scattering intensity curves *sM*(*s*) (experimental—white circles, theoretical—solid lines) for the long and short camera distances (LD and SD) of thiosalicylamide (dynamic model). The difference (experimental – theoretical) curve is shown at the bottom

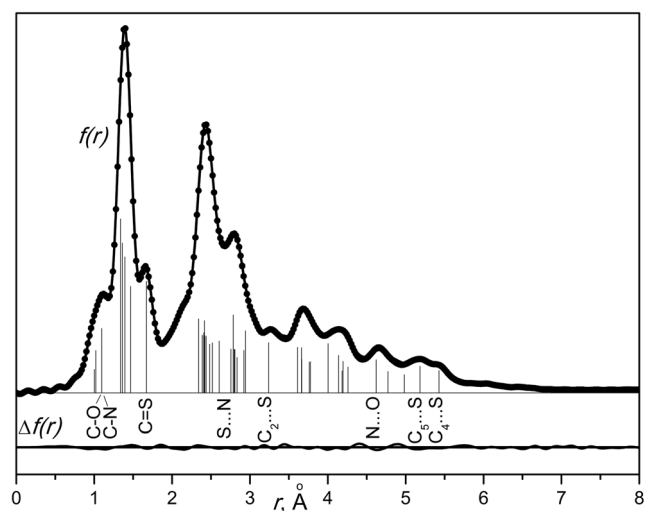


Fig. 7 Radial distribution curves $f(r)$ (experimental—black circles, theoretical—solid line) of thiosalicylamide (dynamic model). The difference (experimental – theoretical) curve is shown at the bottom. Vertical bars indicate relatively important interatomic terms

to the phenol plane. However, the corresponding angular twist of the amide group in salicylamide is $\sim 15^\circ$ (Table 4). These data and the results of NBO analyses reflect the fact that the thioamide moiety is substantially less conjugated with the electron system of the phenol ring than the amide group in salicylamide. Thus, according to NBO analyses, the following weak interactions in thiosalicylamide molecule were revealed: $\sigma(\text{C}1\equiv\text{C}6) \rightarrow \sigma^*(\text{C}=\text{S})$ (stabilization energy $E = 3.5$ kcal/mol), $\sigma(\text{C}=\text{S}) \rightarrow \sigma^*(\text{C}1\equiv\text{C}6)$ ($E = 3.2$ kcal/mol), $\sigma(\text{C}1\equiv\text{C}2) \rightarrow \sigma^*(\text{C}-\text{N})$ ($E = 2.5$ kcal/mol), $\sigma(\text{C}-\text{N}) \rightarrow \sigma^*(\text{C}1\equiv\text{C}2)$ ($E = 2.3$ kcal/mol). On the contrary, in salicylamide molecule, the considerable conjugation is kept even with the distortion from planarity: $\sigma(\text{C}1\equiv\text{C}6) \rightarrow \sigma^*(\text{C}=\text{O})$ ($E = 2.1$ kcal/mol), $\pi(\text{C}1\equiv\text{C}2) \rightarrow \pi^*(\text{C}=\text{O})$ ($E = 27.5$ kcal/mol), $\pi(\text{C}=\text{O}) \rightarrow \pi^*(\text{C}1\equiv\text{C}2)$ ($E = 2.6$ kcal/mol), $\sigma(\text{C}=\text{O}) \rightarrow \sigma^*(\text{C}1\equiv\text{C}6)$ ($E = 1.5$ kcal/mol), $\sigma(\text{C}1\equiv\text{C}2) \rightarrow \sigma^*(\text{C}-\text{N})$ ($E = 2.7$ kcal/mol), $\sigma(\text{C}-\text{N}) \rightarrow \sigma^*(\text{C}1\equiv\text{C}2)$ ($E = 1.5$ kcal/mol).

Table 4 Selected structural parameters of thiosalicylamide, salicylamide, thiobenzamide, and phenol molecules (atom-atom overlap-weighted NAO bond orders are given after the slash symbol)

Parameters ^a	Thiosalicylamide ^b	Thiobenzamide ^c	Salicylamide ^d	Phenol ^e
$r(\text{C}=\text{X})$	1.670(3)/1.18	1.641(4)/1.24	1.232(6)/1.22	
$r(\text{C}-\text{N})$	1.347(12)/1.05	1.352(2)/1.04	1.357(5)/1.04	
$r(\text{C}-\text{C})$	1.463(7)/0.95	1.478(9)/0.90	1.496(4)/0.93	
$r(\text{C}-\text{O})$	1.335(9)/0.94		1.337(5)/0.94	1.381(3)/0.88
X...H	2.07(3)/0.12		1.61(8)/0.10	
$\angle\text{C}_1\text{C}_7\text{X}$	125.6(5)	123.4(5)	120.1(9)	
$\angle\text{C}_2\text{C}_1\text{C}_7\text{X}$	31(3)	31(4)	15(5)	

^a Bond lengths are in Å and bond angles are in degrees

^b Present work, r_e structure

^c Ref. [30], r_e structure

^d Ref. [11], r_{h1} structure

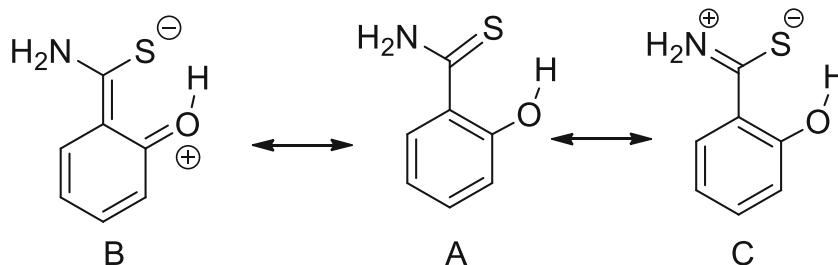
^e Ref. [31], r_g structure

The non-planarity of thiosalicylamide and salicylamide molecules may be caused by the intramolecular repulsion of the two nearby hydrogen atoms: one of the amine group and the other one of the benzene ring (the corresponding H...H distance in the both molecules is about 2.1 Å, whereas van der Waals radius of hydrogen atom is ~ 1.2 Å [32]). The difference in the degree of non-planarity of thiosalicylamide molecule and its oxo-analog is probably connected with different sizes of sulfur and oxygen atoms. The larger radius of sulfur atom causes the angle C1C7S in thiosalicylamide to be $\sim 5^\circ$ bigger than the C1C7O angle in salicylamide (Table 4) that consequently leads to a higher non-planarity thiosalicylamide skeleton in comparison with its oxo-analog.

Comparison of structural parameters of thiosalicylamide with those of related compounds (Table 4) shows that the value of the C=S bond in thiosalicylamide is 0.03 Å longer and the value of the C1–C7 bond is ~ 0.02 Å shorter than in thiobenzamide; the value of the C–O bond in thiosalicylamide is ~ 0.03 Å shorter than the corresponding value in phenol (Table 4). These differences in the bond lengths may be explained by the formation of an intramolecular hydrogen bond O–H...S, which consequently leads to a higher contribution of the resonance form B into the overall structure of thiosalicylamide (see Scheme 1). Thus, the hydrogen bond formation decreases the double bond character of the C=S bond and increases the double bond character of the C1–C7 bond comparing to thiobenzamide, and it also increases the double bond character of the C–O bond comparing to phenol (the corresponding values of the bond orders calculated according Wiberg scheme [33] are presented in Table 4).

The comparison of the numerical values of the S...H distance in S...H–O fragment (2.07(3) Å) and the sum of the van der Waals radii of sulfur atom (1.85 Å [32]) and hydrogen atom (1.2 Å [32]) supports the idea of intramolecular hydrogen bond formation. The S...H distance in thiosalicylamide is by about 0.5 Å longer than the O...H distance in the O...H–O fragment of salicylamide (see Table 4), that fact is in

Scheme 1 Resonance forms of thiosalicylamide.



agreement with the smaller size of oxygen atom (the corresponding van der Waals radius of oxygen atom is 1.4 Å [32]).

NBO analysis confirms the presence of the intramolecular hydrogen bridge as the following stabilization interactions were found: LP1(S) \rightarrow $\sigma^*(\text{O-H})$ ($E = 2.3$ kcal/mol), LP2(S) \rightarrow $\sigma^*(\text{O-H})$ ($E = 25.2$ kcal/mol), $\sigma(\text{C=S}) \rightarrow \sigma^*(\text{O-H})$ ($E = 0.7$ kcal/mol), $\pi(\text{C=S}) \rightarrow \sigma^*(\text{O-H})$ ($E = 1.1$ kcal/mol). The NBO LP2(S) \rightarrow $\sigma^*(\text{O-H})$ orbital overlap diagram representing the O-H...S hydrogen bond is shown in Fig. 8.

The geometry of the six-membered pseudo-ring containing intramolecular hydrogen bond of gaseous thiosalicylamide was found to be quite different from that in the solid phase (see Table 3). In the average, in the gas phase, the C=S bond is ~ 0.02 Å shorter, the C-N bond is ~ 0.04 Å longer and the C-O bond is ~ 0.03 Å longer than corresponding parameters in the crystal. That fact is probably caused by the intermolecular hydrogen bonding in the crystal (see Fig. 9) and as a consequence with higher contribution of resonance form C into the structure of crystalline thiosalicylamide (see Scheme 1).

The intermolecular hydrogen bond formation seems to decrease the double bond character of the C=S bond, causing its elongation, and to increase the double bond character of the C-N bond, causing its shrinkage comparing to the gas phase. The weakening of the intramolecular hydrogen bond caused by the formations intermolecular hydrogen bonds also leads to the elongation of the C-O bond in the solid phase.

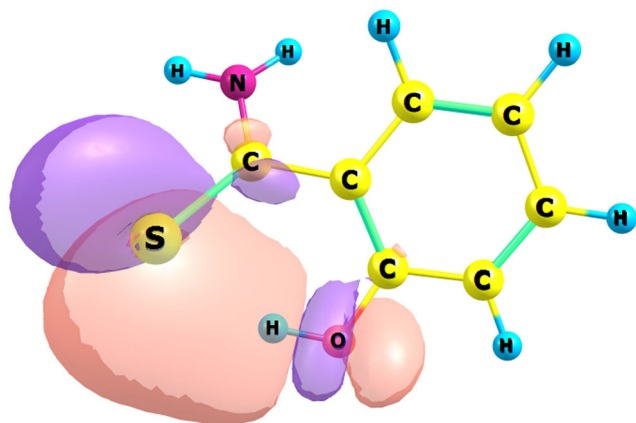


Fig. 8 NBO overlap interaction surface plot (LP2(S) \rightarrow $\sigma^*(\text{O-H})$) reflecting the formation of an intramolecular hydrogen bond in thiosalicylamide

The angle $\text{C}_2\text{C}_1\text{C}_7\text{S}$ turns out to be by about 10° less in the crystal than in the gas phase (Table 3) probably due to the effect of crystal packing as the nearby molecules compensate an interatomic repulsion in a single molecule. The similar difference in the angular twist of the amide group relatively the phenol ring plane is observed for the gaseous and the solid salicylamide ($15 \pm 5^\circ$ in the gas phase [11] versus $2.1 \pm 0.1^\circ$ in the crystal phase [7]).

Concluding remarks

The molecular structure of thiosalicylamide and the internal rotation of the thioamide group were investigated in the gas phase by the joint application of the GED method and QC calculations. According to the obtained results, thiosalicylamide molecule, being free from the intermolecular interactions in the gas phase, exists as a mixture of two non-planar enantiomers with a barrier of their mutual interconversion ~ 1 kcal/mol. The application of GED augmented by QC computations afforded to obtain equilibrium structural parameters of thiosalicylamide as well as parameters of the potential function for the internal rotation of the thioamide group. According to GED, the equilibrium structure of thiosalicylamide in the gas phase is not planar as an interatomic repulsion of nearby hydrogens tries to tilt the thioamide group with respect to the phenol ring. The structural features

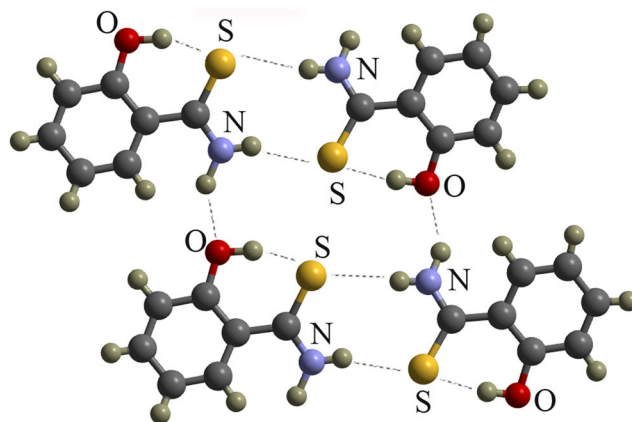


Fig. 9 Hydrogen-bonding motifs observed for thiosalicylamide in the crystal phase

of thiosalicylamide molecule as well as NBO analysis indicate that the conjugation between thioamide group and aromatic ring is almost absent. The existence of intramolecular hydrogen bond was revealed by NBO calculations and the comparison of structural parameters of thiosalicylamide with those of the related molecules. The geometry of gaseous thiosalicylamide was found to be different from that in the solid phase due to the absence of intermolecular hydrogen bonding and the effects of crystal packing in the gas phase.

Acknowledgments The authors express their gratitude to Dr. Ilya I. Marochkin from Lomonosov Moscow State University, Arseniy A. Otlyotov, Dr. Yury A. Zabanov, and Prof. Nina I. Giricheva from Ivanovo State University of Chemistry and Technology for valuable consultations which were very useful for preparing this manuscript.

Funding information This project was made with financial support of the Russian Foundation for Basic Research (Grant Number 18-33-00546 mol_a).

Compliance with ethical standards

Conflict of interest The authors declare that they have no conflicts of interest.

References

- Pospisilova S, Michnova H, Kauerova T, Pauk K, Kollar P, Vinsova J, Imramovsky A, Cizek A, Jampilek J (2018). *Bioorg Med Chem Lett* 28(12):2184–2188. <https://doi.org/10.1016/j.bmcl.2018.05.011>
- Ueda J, Khan ST, Takagi M, Shin-ya K (2010). *J Antibiot* 63(5): 267–269. <https://doi.org/10.1038/ja.2010.26>
- Hardie DG (2013). *Diabetes* 62(7):2164–2172. <https://doi.org/10.2337/db13-0368>
- Mehanna AS, Kim JY (2005). *Bioorg Med Chem* 13(13):4323–4331. <https://doi.org/10.1016/j.bmc.2005.04.012>
- Zhang Y, Mantravadi PK, Jobbagy S, Bao W, Koh JT (2016). *ACS Chem Biol* 11(10):2797–2802. <https://doi.org/10.1021/acscchembio.6b00659>
- Palomar J, De Paz JLG, Catalán J (1999). *Chem Phys* 246(1–3): 167–208. [https://doi.org/10.1016/s0301-0104\(99\)00159-7](https://doi.org/10.1016/s0301-0104(99)00159-7)
- Pertlik F (1990). *Monatsh Chem* 121:129–139. <https://doi.org/10.1007/BF00809525>
- Velcheva EA, Stamboliyska BA (2008). *J Mol Struct* 875(1–3): 264–271. <https://doi.org/10.1016/j.molstruc.2007.04.038>
- Anandan K, Kolandaivel P, Kumaresan R (2005). *Int J Quantum Chem* 104(3):286–298. <https://doi.org/10.1002/qua.20559>
- Manin AN, Voronin AP, Perlovich GL (2013). *Thermochim Acta* 551:57–61. <https://doi.org/10.1016/j.tca.2012.10.013>
- Aarsset K, Page EM, Rice DA (2013). *J Phys Chem A* 117(14): 3034–3040. <https://doi.org/10.1021/jp311003d>
- Banerjee K, Raychaudhury S (1982). *Bull Chem Soc Jpn* 55(11): 3621–3624. <https://doi.org/10.1246/bcsj.55.3621>
- Sambathkumar K (2015). *Spectrochim Acta A* 147:51–66. <https://doi.org/10.1016/j.saa.2015.03.052>
- Jezierska A, Panek JJ, Mazzarello R (2009). *Theor Chem Accounts* 124(5–6):319–330. <https://doi.org/10.1007/s00214-009-0612-2>
- Briel D (2005). *Heterocycles* 65(6):1295–1309
- Kochikov IV, Kovtun DM, Tarasov YI (2008). *Num Meth Program* 9:12–18. http://num-meth.src.msu.ru/zhurnal/tom_2008/pdf/v9r202.pdf. Accessed 13.09.2010
- Frish MJ, Trucks GW, Schlegel HB, Scuseria GE, Robb MA, Cheeseman JR, Zakrzewski VG, Montgomery JA, Stratmann JR, Burant JC, Dapprich S, Millam JM, Daniels AD, Kudin KN, Strain MC, Farkas O, Tomasi J, Barone V, Cossi M, Cammi R, Mennucci B, Pomelli C, Adamo C, Clifford S, Ochterski J, Petersson GA, Ayala PY, Cui Q, Morokuma K, Malick DK, Rabuck AD, Raghavachari K, Foresman JB, Cioslowski J, Ortiz JV, Baboul AG, Stefanov BB, Liu G, Liashenko A, Piskorz P, Komazomi I, Gomperts R, Martin RL, Fox DJ, Keith T, Al-Laham MA, Peng CY, Nanayakkara A, Challacombe M, Gill PM, Johnson B, Chen W, Wong MW, Andres JL, Gonzales C, Head-Gordon M, Replogle ES, Pople JA (2003) *Gaussian 03 (Revision D01)*. Gaussian Inc., Pittsburgh
- Becke AD (1988). *Phys Rev A* 38(6):3098–3000. <https://doi.org/10.1103/PhysRevA.38.3098>
- Lee C, Yang W, Parr RG (1988). *Phys Rev B* 37:785–789. <https://doi.org/10.1103/PhysRevB.37.785>
- Møller C, Plesset MS (1934). *Phys Rev* 46:618–622. <https://doi.org/10.1103/PhysRev.46.618>
- Petersson GA, Bennett A, Tensfeldt TG, Al-Laham MA, Shirley WA, Mantzaris J (1988). *J Chem Phys* 89:2193–2218. <https://doi.org/10.1063/1.455064>
- Dunning TH (1989). *J Chem Phys* 90:1007–1023. <https://doi.org/10.1063/1.456153>
- Weinhold F, Landis CR (2001). *Chem Educ Res Pract* 2:91–104. <https://doi.org/10.1039/B1RP90011K>
- G. A. Zhurko, D. A. Zhurko, *ChemCraft 1.6 build vol. 332* <https://www.chemcraftprog.com/index.html>. Accessed 20.06.2010
- Vishnevskiy YV, UNEX, 2007, **version 1.5**. <http://unexprog.org>. Accessed 2.09.2013
- Ischenko AA, Girichev GV, Tarasov YI (2013) *Electron diffraction: structure and dynamics of free molecules and condensed state of substance*. Fizmatlit, Moscow
- Sipachev VA (2000). *Struct Chem* 11:167–172. <https://doi.org/10.1023/A:1009217826943>
- Vishnevskiy YV, Zhabanov YA (2015). *J Phys Conf Ser* 633: 012076. <https://doi.org/10.1088/1742-6596/633/1/012076>
- Tikhonov DS, Vishnevskiy YV, Rykov AN, Grikina OE, Khaikin LS (2017). *J Mol Struct* 1132:20–27. <https://doi.org/10.1016/j.molstruc.2016.05.090>
- Kolesnikova IN, Putkov AE, Rykov AN, Shishkov IF (2018). *J Mol Struct* 1161:76–82. <https://doi.org/10.1016/j.molstruc.2018.01.084>
- Portalone G, Schultz G, Domenicano A, Hargittai I (1992). *Chem Phys Lett* 197:482–488. [https://doi.org/10.1016/0009-2614\(92\)85804-J](https://doi.org/10.1016/0009-2614(92)85804-J)
- Pauling L (1960) *The nature of the chemical bond* 3rd edn. Cornell University Press, Ithaca
- Wiberg KB (1968). *Tetrahedron* 24:1083–1196. [https://doi.org/10.1016/0040-4020\(68\)88057-3](https://doi.org/10.1016/0040-4020(68)88057-3)

Publisher's note Springer Nature remains neutral with regard to jurisdictional claims in published maps and institutional affiliations.